FRAGMENT SIZE DETECTION WITHIN HOMOGENEOUS MATERIAL USING GROUND PENETRATING RADAR

Allen Benter, Richard Xu, Wayne Moore, Michael Antolovich, Junbin Gao
Centre for Research into Complex Systems
Charles Sturt University
Bathurst, Australia
abenter@csu.edu.au

***Abstract*—Ground Penetrating Radar (GPR) offers the ability to observe the internal structure of a pile of rocks. Large fragments within the pile may not be visible on the surface. Determining these large fragment sizes before collection can improve mine productivity. This research has examined the potential to identify objects where the background media and the object exhibit the same dielectric properties. Preliminary results are presented which show identification is possible using standard GPR equipment.**

***Index Terms*—Ground Penetrating Radar; dielectric properties; Fragmentation sizing**

I. Introduction

The ability to determine the size of rock fragments before crushing is needed in all mines employing secondary breakage. In a typical mining scenario, large fragments entering crusher units have the potential to block the crusher, preventing subsequent loads from being processed. This blockage reduces overall productivity of the mine.

Fragment size detection prior to the crushing stage is generally only possible at the draw point after blasting and in the Load Haul/Dump (LHD) vehicle while being transported to the crusher. Presently the driver of the extraction vehicle is the primary means to prevent large fragments entering the system, visually inspecting the draw point for any fragments that would be too large for the crusher. This inspection is only able to determine the presence of large fragments clearly visible on the surface of the pile.

For efficient processing, we require a decision to be made about whether a large fragment is present before the load enters the crusher unit. Ideally this would be made at the draw point. GPR gives us the ability to observe beneath the surface of the rock pile. Electromagnetic waves propagate through the material and are reflected off changes in the electrical characteristics within the ore. These can occur with the presence of conductive materials or where the material changes, such as the presence of a void within the pile [1].

The main civilian uses of GPR are in the areas of archaeological discovery, non destructive testing and engineering examination of soils. GPR has also been used to detect land mines. Within the mining industry there has been research into using GPR to discover the extent of coal seams to enable efficient extraction of coal. The authors of [2] have achieved high resolution of the seam horizon depth down to about 5mm accuracy. The mining application we are investigating is looking for areas where there is no interruption to the base material, hence if one reflection masks another it will be unlikely to disguise the presence of the large fragment [3].

Most research into GPR has observed a contrast between the dielectric properties of the object of interest and a different, homogeneous background medium. Reference [3] investigated the resolution of GPR in archaeological surveys, embedding concrete objects in a sand box. Similarly, [4] used GPR to identify small objects representing land mines, again embedded in sand. In both cases, the material was uniformly packed around the objects, although [3] was able to detect different grain size accumulation as a result of excavation and placement of objects. When there is little or no contrast between the object and background, identification of individual objects becomes more difficult. A profile of railway ballast exhibits little contrast between the ballast and sub-ballast, making identification of ballast fouling very difficult [5].

Our literature review does not identify any other research using GPR to detect fragmentation rates beneath the surface of a rock pile. The following sections will present results of using GPR to detect the presence of large fragments within the structure of a pile of rocks. The rest of the paper is organized as follows: Section II will describe some background information in mining process and optical fragmentation systems; Section III and IV will discuss data collection and data processing, respectively; and Section V will then look at further work that

This work was funded by Newcrest Mining Ltd (www.newcrest.com.au). Additional support has been received from Alpha GeoScience Pty Ltd (Aust.) (www.alpha-geo.com).

will be conducted as part of this research program.

II. BACKGROUND

After blasting, the fragmented ore is collected by a LHD and taken to the crusher unit for secondary breakage. If a fragment deemed too large for the crusher is observed at the draw point, the driver will then abort the collection and close the tunnel until the fragment is broken further. A secondary crusher team is then sent to the tunnel to break the large fragment in-situ and enable the tunnel to be re-opened.

Automatic detection of fragment sizes has been researched at the draw point, during collection (in the LHD) and after crushing. The opportunities to capture images are limited to a few locations within the mining process. After blasting, the material remains at the draw point until collection. The fragmentation of rocks is most difficult to be determined at this point due to the irregular surfaces of the pile that is presented to the capture device. Once collected by a LHD, the material is confined within the bucket, and can be captured either by a vehicle mounted camera or at a common image collection point which the vehicles pass on their way to the crusher [6].

A number of commercial software packages exist to determine fragment size distribution. A comparison of manual image analysis and software image analysis was undertaken in [7], where it was found that the results were not consistent between the competing packages. After merging a number of photographs together, one of the packages produced results comparable to the manual methods. However, it was also noted that manual analysis was very time consuming, and the software packages required additional manual editing to improve the results.

The techniques described in [8] captures images of fragments within a feed chute to dual crusher units, manually filtering the stream of fragments entering the chute using heavy steel chains. These measures reduce the stream to a single layer, enabling the computer vision system to identify any fragments capable of blocking the crusher. If such a fragment is present in one of the chutes leading to the two crushers, that crusher unit can be shutdown to enable secondary breaking without interrupting the other crusher.

Further image capture is possible post-crusher stage. However these scenarios are outside the scope of this paper.

Current semi-autonomous vehicles send streaming video to a remote tele-operator who makes the determination regarding the size of the fragments prior to collection. The major problem with optical images, is that the images only show the surface of the pile. Any large fragments that are partially or fully obscured by surface fragments will be undetectable. The authors of [9] have developed a probability model of a laboratory pile to determine the internal structure of the pile. This method however relies on prior knowledge of the composition of the pile fragment size distribution.

Computer vision systems can also experience extrinsic problems. An underground mining environment, complete with explosives and heavy vehicles, is a dark and dusty place. Using standard lighting, ore dust and vehicle emission particulate matter can prevent the capture of clear images that would enable determination of the surface fragment size. Camera systems mounted on mining vehicles also suffer from the vibrations of motion and engine operation, affecting camera calibration [10], [11]. A detailed discussion of the inherent errors in optical image capture is described in [12].

Research is continuing into autonomous operations of mining vehicles [13]. One obstacle to fully-autonomous vehicles is the detection of oversize fragments presenting at the draw point with the potential to block the primary crusher. Techniques to determine fragment sizes have relied upon the large fragment being visible at the surface of the rock pile, however this is not always the case. A detection system that could penetrate the surface of the fragment pile and determine the presence of over sized fragments could assist the remote operators and autonomous vehicle operation in avoiding the collection of large fragments.

III. DATA COLLECTION

The experiments discussed in this paper represent the first phase of experiments to detect the degree of fragmentation in a pile of rocks. The outcomes were established to use GPR to identify a large fragment (single rock) within a collection of smaller fragments. To achieve this, experiments were designed to enable data collection within the laboratory, in consideration of the handling of materials.

The material investigated consisted of granite ore interspersed with minute particles of gold (about 2g per tonne) and copper (about 6.6kg per tonne). The project sponsor provided approximately 300kg of rock of various sizes ranging from about 10mm to 80mm in diameter. A single fragment measuring approximately 250mm (surface diameter) x 130mm (h) was also provided.

A. Experimental Setup

Based on the reported dielectric properties of granite [14], it was assumed the propagation speed of the signal through the material would be 130mm/ns. Using this assumption the wavelength, vertical resolution and Fresnel zone at various depths were calculated (see Table I).

The first column shows various frequencies of standard GPR antennas. The vertical resolution (column 2) was determined as one-quarter of the wavelength of the frequency [REF]. Horizontal resolution, or radar footprint, is determined by the Fresnel zone, according to equation 1 [14]

$$A = \frac{\lambda}{4} + \frac{D}{\sqrt{\epsilon_r}} \tag{1}$$

Table I
VERTICAL AND HORIZONTAL RESOLUTION OF VARIOUS WAVELENGTHS

$f(GHz)$	$\frac{\lambda}{4}$	A	$\frac{A}{2}$
0.5	0.067	0.268	0.134
1.0	0.034	0.238	0.119
1.2	0.028	0.232	0.116
1.6	0.021	0.225	0.112

where

A = footprint length along the path of the antenna
λ = wavelength
D = depth (0.5m)
ϵ_r = dielectric constant

Based on the sizes of the available ore samples, it was decided that a frequency of approximately 1GHz would allow resolution of the large fragment horizontally. A Mala Geoscience 1.2GHz antenna and CX11 Concrete imaging system was used for these experiments. A plywood box with internal dimensions of 570 x 570 x 570mm was constructed (without metal screws or strapping) to hold the samples under controlled conditions. A wooden track was constructed to sit over the top of the box, upon which the antenna was moved above and across the box and rock fragments to obtain horizontal scans.

B. Calculating propagation speed

The first experiment is to scan the empty box. This revealed a significant reflection returned at 4.1ns, after correcting for zero-offset. Calculating the distance to the reflected object (using velocity 0.3m/ns), corresponded with the base of the box and the offset to the antenna base when mounted on the frame.

The next set of experiments was to confirm the propagation speed of the signal through the sample ore. The rock material was placed in the bottom of the box. To enable efficient handling of the material, the loose fragments were contained within cotton bags which, when packed, measured approx. 400mm x 250mm area x 150mm high. These bags were then placed in the box on top of each other to achieve a single column of fragments measuring about 400mm x 250mm area x 450mm high.

Over a series of experiments, the rock bag column was built up using 1, 2 and 3 bags of ore. A comparison of the average signal values enabled detection of the top of the column in each experiment. Further comparison with a scan over the empty box enabled the determination of the bottom of the box. Figure I (top to bottom) shows the signal returns for the scans over the empty box; large rock; and bagged fragments in columns of 1 bag; 2 bags and 3 bags. The horizontal axis shows signal return time (ns) and the vertical axis shows the signal amplitude. From the top and bottom time values it was possible to calculate the time of travel, and hence, the propagation speed through the rocks. The results of these experiments are shown in Table II.

C. Scanning a column of fragments

The next set of experiments were structured to detect the presence of a larger rock fragment. The columns under examination consisted of (a) three bags of fragments; (b) a large rock between two bags of fragments; (c) a large rock completely surrounded (top, bottom, sides) by bagged fragments. Each of the scans was obtained using the antenna in motion. The data was then processed using MatGPR [15].

IV. DATA PROCESSING

Based on the propagation speed through the solid fragment and the bagged materials, it was possible to determine the size of each component in the scan. Hence, with each scan the location of the bagged material or the single fragment could be determined based on the signal time.

Data from each scan was imported into MatGPR and processed using the standard routines available. The processing of the data involved the following steps: (i) import raw data; (ii) background removal; (iii) instantaneous amplitude. The results of the three scans (a), (b) and (c) are shown in Figures 2, 3 and 4 (respectively).

Figure 2 shows the initial scan over three bags of fragments. The centre line of the column is located at approximately 0.35 metres along the scan axis. There is a large return of signal early in the scan, representing returns from the top bag. The second bag located approximately between 2-4 ns reflects from the leading and trailing edges, evidenced by the returns at 2-3ns starting from about 0.05m to 0.65m. The contents of the bag (0.2m-0.45m) are delineated with two distinct bright points at 2.5ns (0.28m and 0.4m) separated by voids. Below the second bag, the only significant returns are from the leading and trailing edges of the third bag.

The result of the next scan is shown in Figure 3: a similar leading noise identifying the top bag of fragments. The large rock is located between 2-4ns, with the leading and trailing edge of the rock visible. In comparison with Figure 2, the reflections between 2-3ns are not saliently evident. Of interest is the relatively large and contiguous zone between these points representing the volume of the single rock. Also of note is the return showing the top of the second bag located beneath the large rock.

The final scan, Figure 4, represents the large rock tightly surrounded by bagged fragments. In this figure the top bag is evident at the top of the scan. The centre, contiguous zone in the figure (0.35m, 3ns) is the location of the large rock. Some reflections are evident below the rock.

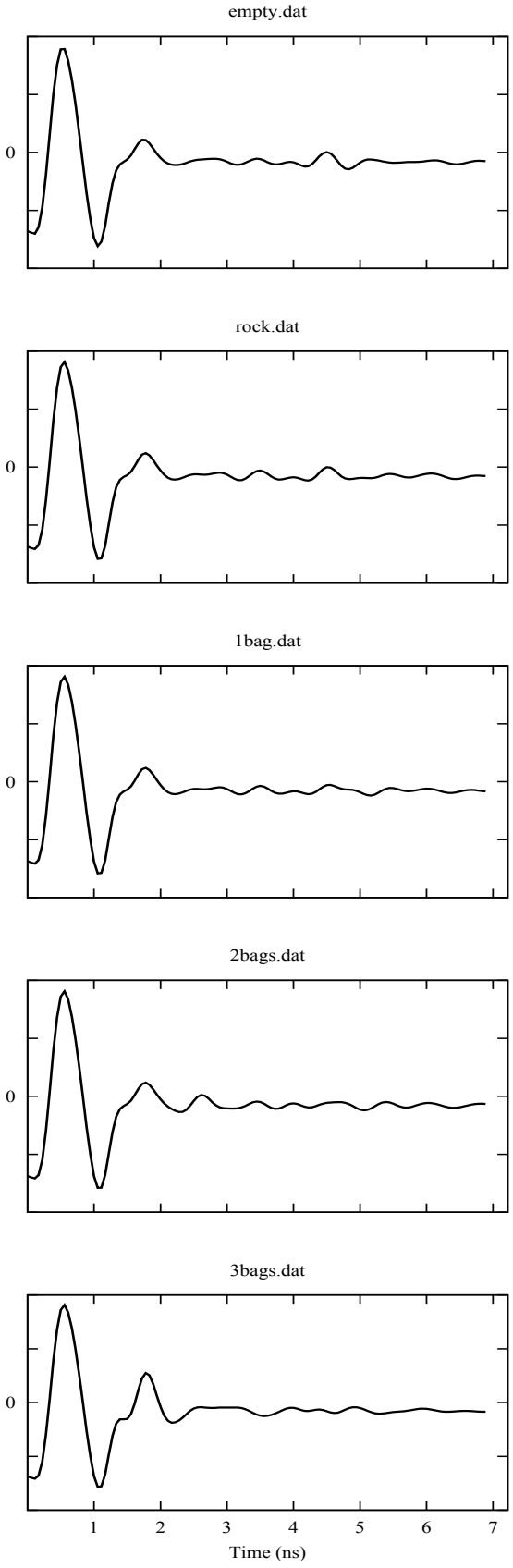

Figure 1. Scans over samples in wooden box

Table II
CALCULATION OF PROPAGATION SPEED THROUGH ORE SAMPLES

	Rock	1 Bag	2 Bags	3 Bags	Cumm.
Top (ns)	3.32	3.32	2.33	1.39	-
Bottom (ns)	5.26	4.93	5.15	5.71	-
Time Diff. (ns)	1.94	1.61	2.83	4.32	8.75
Distance (m)	0.13	0.14	0.28	0.42	0.84
Propagation (m/ns)	0.13	0.18	0.20	0.19	0.19

Figure 2. Scan image over three bags of small fragments

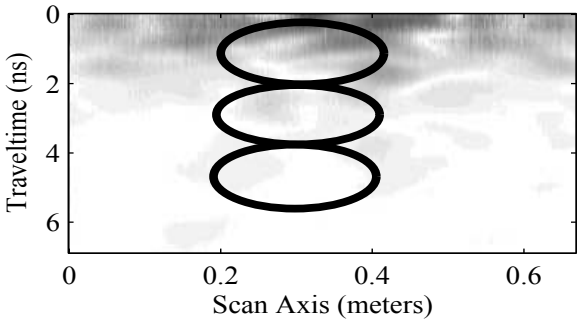

Figure 3. Scan image over large rock placed between two bags of smaller fragments

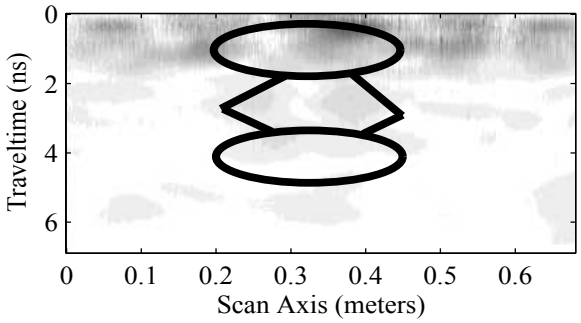

Figure 4. Scan image over large rock surrounded by bags of smaller fragments

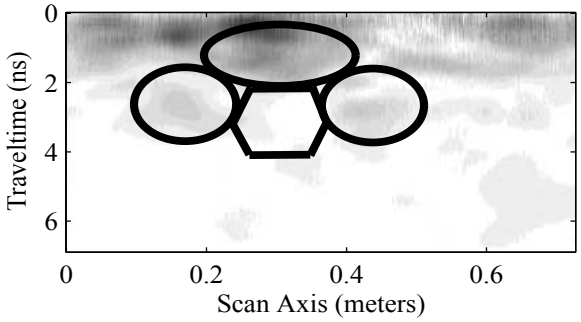

V. Discussion

The scans over the columns of rock fragments show it is possible to differentiate rock fragments of different sizes under controlled conditions. The position of a large fragment within a column of smaller fragments could be determined using the return signal amplitude. Also of significance was the depth of penetration, where a deeper penetration indicated the possible presence of a large fragment in the upper path of the trace.

Initial experiments confirmed the propagation speed through the single rock and bagged fragments indicated there exists a difference in propagation speed between solid rock and smaller fragments of the same material. It may be possible in future experiments to exploit this difference to identify and size fragments identified in a group of GPR traces. The results of these experiments are encouraging. Future experiments will use larger rock fragments and various antenna frequencies to confirm the details in this paper.

References

[1] M. Richards, *Fundamentals of Radar Signal Processing*. McGraw Hill, 2005.

[2] A. Strange, J. Ralston, and V. Chandran, "Near-surface interface detection for coal mining applications using bispectral features and gpr," *Subsurface Sensing Technologies and Applications*, vol. 6, no. 2, pp. 125–149, 2005.

[3] J. Leckebusch and R. Peikert, "Investigating the true resolution and three-dimensional capabilities of ground-penetrating radar data in archaeological surveys: Measurements in a sand box," *Archaeological Prospection*, no. 8, pp. 29–40, 2001.

[4] H. Herman, "Robotic subsurface mapping using ground penetrating radar," Ph.D. dissertation, Carnegie Mellon University, May 1997.

[5] R. Roberts, I. Al-Qadi, J. Tutumluer, E. Boyle, and T. Sussmann, "Advances in railroad ballast evaluation using 2ghz horn antennas," *Proceedings of the 11th International conference in Ground Penetrating Radar*, 2006.

[6] N. Maerz and T. W. Palangio, "Post-muckpile, pre-primary crusher, automated blast fragmentation sizing," *The International Journal for Blasting and Fragmentation*, vol. 8, no. 2, 2004.

[7] J. Sudhakar, G. R. Adhikari, and R. N. Gupta, "Technical note: comparison of fragmentation measurements by photographic and image analysis techniques," *Journal of Rock Mechanics and Rock Engineering*, vol. 39, no. 2, pp. 159–168, 2006.

[8] E. Cabello, M. A. Sanchez, and J. Delgado, "A new approach to identify big rocks with applications to the mining industry," *Real-Time Imaging*, vol. 8, pp. 1–9, 2002.

[9] M. Thurley, "Three dimensional data analysis for the separation and sizing of rock piles in mining," Ph.D. dissertation, Monash UIniversity, 2002.

[10] Z. Zhang, "Flexible camera calibration by viewing a plane from unknown orientations," in *International Conference on Computer Vision*, 1999, pp. 666–673.

[11] N. Maerz and W. Zhou, "Calibration of optical digital fragmentation measuring systems," *The International Journal for Blasting and Fragmentation*, vol. 4, no. 2, pp. 126–138, 2000.

[12] N. Maerz and W. Zhou, "Optical digital fragmentation measuring systems inherent sources of error," *The International Journal for Blasting and Fragmentation*, vol. 2, no. 4, pp. 415–431, 1998.

[13] P. Ridley and P. Corke, "Autonomous control of an underground mining vehicle," in *Australian Conference on Robotics and Automation*, 2001, pp. 26–31.

[14] A. P. Annan, "Ground penetrating radar workshop notes," Tech. Rep., 2001.

[15] A. Tzanis, "Matgpr: A freeware matlab package for the analysis of common-offset gpr data," *Geophysical Research Abstracts*, vol. 8, no. 09448, 2006.